

# A Theranostic Small Interfering RNA Nanoprobe Protects Pancreatic Islet Grafts From Adoptively Transferred Immune Rejection

Ping Wang,<sup>1</sup> Mehmet V. Yigit,<sup>1</sup> Chongzhao Ran,<sup>1</sup> Alana Ross,<sup>1</sup> Lingling Wei,<sup>2</sup> Guangping Dai,<sup>1</sup> Zdravka Medarova,<sup>1</sup> and Anna Moore<sup>1</sup>

Islet transplantation has recently emerged as an acceptable clinical modality for restoring normoglycemia in patients with type 1 diabetes mellitus (T1DM). The long-term survival and function of islet grafts is compromised by immune rejection-related factors. Downregulation of factors that mediate immune rejection using RNA interference holds promise for improving islet graft resistance to damaging factors after transplantation. Here, we used a dual-purpose therapy/imaging small interfering (si)RNA magnetic nanoparticle (MN) probe that targets  $\beta_2$  microglobulin (B2M), a key component of the major histocompatibility class I complex (MHC I). In addition to serving as a siRNA carrier, this MN-siB2M probe enables monitoring of graft persistence noninvasively using magnetic resonance imaging (MRI). Human islets labeled with these MNs before transplantation into B2M (null) NOD/*scid* mice showed significantly improved preservation of graft volume starting at 2 weeks, as determined by longitudinal MRI in an adoptive transfer model ( $P < 0.05$ ). Furthermore, animals transplanted with MN-siB2M-labeled islets demonstrated a significant delay of up to  $23.8 \pm 4.8$  days in diabetes onset after the adoptive transfer of T cells relative to  $6.5 \pm 4.5$  days in controls. This study demonstrated that our approach could protect pancreatic islet grafts from immune rejection and could potentially be applied to allotransplantation and prevention of the autoimmune recurrence of T1DM in islet transplantation or endogenous islets. *Diabetes* 61:3247–3254, 2012

**T**ype 1 diabetes mellitus (T1DM) is characterized by the selective and progressive destruction of pancreatic  $\beta$ -cells, leading to insulin dependency and serious complications (1). Pancreatic allotransplantation offers superior glycemic control for T1DM patients and can prevent or even reverse secondary complications (2). However, this procedure is associated with significant mortality and morbidity (3).  $\beta$ -Cell replacement by islet transplantation provides a less invasive alternative T1DM treatment, with reduced antigen load, relative surgical simplicity, and low morbidity (4). Unfortunately, even with the success of the Edmonton immunosuppressive protocol, only 20% of patients remained insulin-independent

3 years after islet transplantation (5). Studies indicate that several factors influence the decrease in islet graft function (6). Among them are immunologic factors that play a critical role because they contribute to innate and adaptive immune rejection (7), recurrence of autoimmunity (8), and toxicity associated with immunosuppressive agents (9,10).

The potential for islet grafts to elicit allo- or xenoinnogenic responses depends on their major histocompatibility complex (MHC) compatibility with the recipient HLA (11). Alloreactivity is significantly reduced in HLA-matched islet transplantation (12); however, limited sources of donor islets and extensive HLA polymorphisms restrict HLA-matched allotransplantation (13), prompting the search for alternative transplant sources.

One approach involves the use of xenografts (14), although significant immunologic barriers must be overcome before xenotransplantation becomes a reality in a clinical setting (15). As such, a T cell-mediated immune response occurring within weeks or even days of grafting causes irreversible  $\beta$ -cell damage (16). Major immune contributors to this damage include cytotoxic cluster of differentiation (CD)8<sup>+</sup> T cells that recognize antigenic peptides in context with MHC class I molecules in allo- and xenografts (17,18). Reduction or downregulation of MHC class I protein expression using RNA interference (RNAi) (19) has shown some success in overcoming the limitations of immune rejection in cell-based therapies. The delivery of short hairpin RNA to HeLa cells resulted in a selective and permanent silencing of MHC class I by up to 90%, even under inflammatory conditions (20). MHC class I knock-down was effective in preventing antibody-mediated cell lysis and CD8<sup>+</sup> T cell response (20). Lentivirus-mediated silencing of HLA in human 293 cells promoted resistance to killing by alloreactive T-effector cells (21) and showed enhancement in hematopoietic stem cell transplantation (22). Encouraged by these results, we sought to use RNAi to disturb MHC class I expression in human islet cells through the silencing of  $\beta_2$  microglobulin (B2M), a key component of MHC class I molecules, thereby reducing graft rejection in a model of xenotransplantation.

Because a safe and highly efficient delivery method is essential for the eventual clinical application of RNAi in islet grafts, we used magnetic nanoparticles (MNs) as a delivery vehicle for B2M small interfering (si)RNA into islet cells. This approach was selected rather than viral vector nucleotide delivery because it is not undermined by excessive inflammation (23) or the potential for oncogenicity (24). In addition to serving as a siRNA carrier, the MNs enable the monitoring of graft persistence noninvasively using magnetic resonance imaging (MRI) (25,26). Treatment of human islets with these dual-purpose

From the <sup>1</sup>Molecular Imaging Laboratory, MGH/MIT/HMS Athinoula A. Martinos Center for Biomedical Imaging, Department of Radiology, Massachusetts General Hospital, Harvard Medical School, Boston, Massachusetts; and the <sup>2</sup>Transplantation Biology Research Center, Massachusetts General Hospital, Harvard Medical School, Boston, Massachusetts.

Corresponding author: Anna Moore, amoore@helix.mgh.harvard.edu.

Received 9 April 2012 and accepted 15 June 2012.

DOI: 10.2337/db12-0441

This article contains Supplementary Data online at <http://diabetes.diabetesjournals.org/lookup/suppl/doi:10.2337/db12-0441/-DC1>.

© 2012 by the American Diabetes Association. Readers may use this article as long as the work is properly cited, the use is educational and not for profit, and the work is not altered. See <http://creativecommons.org/licenses/by-nc-nd/3.0/> for details.

See accompanying commentary, p. 3068.

therapeutic/imaging MNs before transplantation resulted in significantly improved survival of grafts and a delay in the onset of hyperglycemia after the adoptive transfer of T cells to animals with newly established xenografts. Our approach provides for protection of transplanted islet grafts and can be potentially extended for various transplantation and cell therapy applications.

## RESEARCH DESIGN AND METHODS

**Probe synthesis and characterization.** The synthesized probe consisted of magnetic dextran-coated iron oxide MNs labeled with Cy5.5 near-infrared optical dye and conjugated to siRNA at the dextran surface. First, we synthesized Cy5.5-labeled MNs, as previously reported (27). Briefly, a solution of monoactivated Cy5.5 succinimide ester (Amersham Biosciences, Piscataway, NJ) in 20 mmol/L sodium citrate and 0.15 mol/L NaCl was reacted with previously dialyzed immunopure, aminoderivatized dextran-coated iron oxide (pH 8.5) with constant agitation for 12 h at room temperature. The Cy5.5-labeled aminated iron oxide (MN-Cy5.5) was purified from unreacted dye using a Sephadex G-25, PD-10 column (Amersham Biosciences). MN-Cy5.5 was then conjugated to the heterobifunctional cross-linker *N*-succinimidyl 3-(2-pyridyldithio) propionate (SPDP; Pierce Biotechnology, Rockford, IL) by means of the *N*-hydroxy succinimide ester, followed by purification using a Sephadex G-25, PD-10 column in PBS/EDTA (pH 7.5). The number of SPDP molecules per crystal was determined based on the release of pyridine-2-thione at 343 nm ( $\epsilon = 8.08 \times 10^3$  mol/cm) after the addition of 35 mmol/L of the reducing agent, tris-(2-carboxyethyl) phosphine hydrochloride (TCEP, Thermo Fisher Scientific, Rockford, IL) in DMSO. A ratio of 16 SPDP molecules per nanoparticle was obtained. The size of the MNs was  $34.26 \pm 0.29$  nm with a polydispersity index (PDI) of 0.22. The  $\zeta$  potential at pH 7.00 was  $+16.8 \pm 2.65$  mV.

Double-stranded siRNA targeting human *B2M* (NM 004048.2) and scrambled (SCR) siRNA were synthesized by Dharmacon (Lafayette, CO). The siRNAs were modified to incorporate a thiol group on the 5' end of the sense strand. The disulfide protecting groups on 5'-S-S- were deprotected using TCEP according to the manufacturer's instructions. The *B2M*-targeting and scrambled siRNA duplexes were then conjugated to MN-Cy5.5-SPDP through the 5'-sense thiol group. The siRNA was reacted overnight (4°C) with the previously activated MN-Cy5.5-SPDP product via the SPDP cross-linker in PBS/EDTA (pH 8), followed by purification using a Quick Spin Column G-50 Sephadex Column (Roche Applied Science, Indianapolis, IN; Supplementary Fig. 1).

The resulting *B2M*-targeting and scrambled probes, designated MN-siB2M and MN-siSCR, respectively, were purified using magnetic separation columns (Miltenyi Biotec, Inc., Auburn, CA). The amount of conjugated siRNA was assayed using agarose gel electrophoresis. The amount of siRNA dissociated from the nanoparticles was assessed under reducing conditions by pretreatment with 15 mmol/L TCEP for 30 min. siRNA standards, untreated probes, and probes treated with a reducing agent were applied to a 2% agarose gel in TBE buffer (Invitrogen, Carlsbad, CA) and run at 145 V for 1 h. The gel was stained with 0.5  $\mu$ g/mL ethidium bromide (Sigma-Aldrich, St. Louis, MO) for 30 min, and visualized using a Molecular Imager FX scanner (Bio-Rad Laboratories, Hercules, CA). On average, the conjugation resulted in 1.8 pmol siRNA/ $\mu$ g Fe (Supplementary Fig. 2).

**Human islet culture and islet treatment with probe.** Human islets were obtained from the Integrated Islet Distribution Program (IIDP Centers, National Institutes of Health and Juvenile Diabetes Research Foundation). The viability and purity of the islets exceeded 85%. On arrival at our facility, islets were cultured in 24-well nontreated plates (Nunc, Roskilde, Denmark) at 1,000 islet equivalents (IEQ)/well in CMRL 1066 medium (GIBCO, Grand Island, NY) supplemented with 10% FBS and 100  $\mu$ g/mL penicillin-streptomycin.

To mimic activated conditions, the upregulation of MHC class I molecules was accomplished by stimulation of human islets with 50 ng/mL recombinant human interferon (IFN)- $\gamma$  (R&D Systems, Minneapolis, MN) for 48 h (28). For labeling experiments, 1000 IEQ were incubated with MN-siB2M or MN-siSCR for 48 h in the IFN- $\gamma$ -containing medium (25  $\mu$ g Fe, 45 pmol siRNA, in 1 mL medium).

**Splenocyte isolation and islet protein-stimulated enzyme-linked immunosorbent spot (ELISPOT).** For the islet protein-stimulated ELISPOT, total splenocytes isolated from NOD mice 4–6 weeks of age (The Jackson Laboratory, Bar Harbor, ME) were restimulated by incubation with sonicated islet proteins (5  $\mu$ g/mL) or phorbol 12-myristate 13-acetate (PMA, Sigma-Aldrich, St. Louis, MO, 50 ng/ml) for 7 days (29). No stimulator was added to the mock controls. The CD8<sup>+</sup> T cells were isolated from each group with a CD8a<sup>+</sup> T Cell Isolation Kit (Miltenyi Biotec, Inc., Auburn, CA). The purity of the CD8<sup>+</sup> T cells was evaluated by fluorescence-activated cell sorter (FACS) with PE-labeled rat anti-mouse CD8 monoclonal antibody (BD Biosciences, Bedford, MA) and fluorescein isothiocyanate (FITC)-labeled anti-mouse CD3 monoclonal antibody

(Cedarlane Laboratories, Hornby, ON, Canada). The separated CD8<sup>+</sup> T cells were seeded at  $2 \times 10^5$ /well in ELISPOT plates and incubated with islet proteins for another 48 h. The release of IFN- $\gamma$  was assessed by ELISPOT according to the manufacturer's protocol (R&D Systems, Inc.). The results were expressed as spot counts/ $2 \times 10^5$  CD8<sup>+</sup> T cells.

**Islet transplantation and adoptive transfer of splenocytes for induction of immunorejection.** All animal experiments were performed in compliance with institutional guidelines and approved by the subcommittee on research animal care at Massachusetts General Hospital.

The recipients were 5-week-old B2M-deficient (null) NOD/*scid* mice ( $n = 22$ ; The Jackson Laboratory). Diabetes was induced by intraperitoneal injection of streptozotocin (STZ; 200 mg/kg body weight; Sigma-Aldrich) freshly dissolved in Na citrate buffer (30). Diabetes was confirmed by weight loss, polyuria, and blood glucose levels higher than 250 mg/dL. MN-siB2M-labeled human pancreatic islets were implanted under the left kidney capsule (1,500 IEQ/kidney) of B2M (null) NOD/*scid* mice ( $n = 10$ ). For the control group, the same number of MN-Cy5.5-labeled islets was transplanted under the left kidney capsule of B2M (null) NOD/*scid* mice ( $n = 10$ ).

Normoglycemia was restored in all animals 2–3 days after transplantation. To induce immune rejection, 1 week after transplantation,  $5 \times 10^6$  splenocytes isolated from 8-week-old NOD mice (The Jackson Laboratory) were adoptively transferred to experimental and control mice intravenously. Two 5-week-old B2M (null) NOD/*scid* mice transplanted with MN-siB2M-labeled human pancreatic islets did not receive the splenocyte injection and served as a “no adoptive transfer” control group.

**In vivo optical imaging.** All animals were fed an alfalfa-free diet (TestDiet, Richmond, IN) 2 weeks before islet transplantation. In vivo optical imaging was performed using a whole-body animal imaging system (IVIS Spectrum, Caliper Life Sciences, Hopkinton, MA), equipped with 10 narrow-band excitation filters (30-nm bandwidth) and 18 narrow-band emission filters (20-nm bandwidth). The Cy5.5 signal from the recipient mice was collected at 640 nm excitation and 720 nm emission. To validate the origin of the Cy5.5 signal in the animals, three-dimensional (3D) reconstruction was performed using Living Image 4.2 software (Caliper Life Sciences, Hopkinton, MA).

**In vivo MRI of transplanted human islet grafts.** In vivo MRI was done using a 9.4-T scanner with a Bruker Biospin Avance Console equipped with ParaVision 5.1 software on 1, 7, 14, 21, 27, 35, and 42 days after adoptive transfer. Imaging protocols consisted of T2-weighted spin echo, T2\*-weighted gradient echo, and multislice multiecho T2 map. T2-weighted images were analyzed on a voxel-by-voxel basis by fitting the T2 measurements to a standard exponential decay curve, defined by the equation:  $[y = A \exp(-t/T2)]$  (31). We calculated graft volumes by counting the number of voxels in each slice of a region of interest (ROI) surrounding the graft and multiplying by voxel volume (0.05 mm<sup>3</sup>) using Marevis 3.5 software (Institute for Biomedicine, National Research Council, Canada). To assess graft survival, blood glucose levels of experimental and control mice were monitored using a Accensia Contour Blood Glucose Monitoring System (Bayer Health Care, Tarrytown, NY) twice weekly starting before STZ injection and extending 6 weeks after adoptive transfer.

### Histology and fluorescence microscopy

**In vitro studies.** In vitro labeling of human islets with MN-siRNA probes was confirmed by histologic analysis. After incubation for 48 h with the probes, the islets were fixed in 4% formaldehyde, embedded in paraffin, sectioned, and stained with Prussian blue to identify the presence of iron in labeled islets. Briefly, sections were immersed in Prussian blue solution containing 5% potassium ferrocyanide (ACROS Organics, Fairlawn, NJ) and 5% hydrochloric acid (Aldrich, Milwaukee, WI) for 30 min and counterstained with nuclear fast red (Sigma-Aldrich).

For fluorescence microscopy, islet sections were incubated with mouse monoclonal antibody to dextran (1:100 dilution; Stemcell Technologies, Vancouver, BC, Canada) at 4°C overnight, followed by an FITC-labeled goat anti-mouse IgG secondary antibody (1:100 dilution, Invitrogen). After incubation, slides were mounted with a mounting medium containing DAPI (Vectashield, Vector Laboratories, Inc., Burlingame, CA). Images were acquired on a Nikon Eclipse 50i microscope using a SPOT 7.4 Slider RTKE CCD camera (Diagnostic Instruments, Sterling Heights, MI) and analyzed with iVision 4.015 software.

To demonstrate B2M downregulation after incubation with the probes, in vitro islets were treated as described above, and islet sections were incubated with rabbit polyclonal antibody to B2M (1:500 dilution; Abcam) at 4°C overnight, followed by incubation with fluorescein-labeled anti-rabbit IgG (H+L; 1:200 dilution, Vector Laboratories, Inc.). After incubation, slides were mounted with a medium containing DAPI, as described above.

**In vivo studies.** Mice from the experimental and control group ( $n = 2$ ) were killed 2 weeks after adoptive transfer. Their left kidneys were removed, embedded in paraffin, and cut into 5- $\mu$ m sections. After antigen retrieval with Tris-EDTA buffer (pH 8.0) in the microwave oven for 10 min, tissue sections

were blocked in 5% normal goat serum in PBS. For human insulin and mouse CD8<sup>+</sup> T cells double-staining, sections were incubated with a guinea pig anti-human insulin primary antibody (1:200 dilution, Abcam) and rat anti-mouse CD8 monoclonal antibody (1:50 dilution, Abcam), followed by an FITC-labeled goat anti-guinea pig secondary IgG (1:100 dilution, Abcam) and Alexa Fluor 594 conjugated secondary goat anti-rat IgG (1:50 dilution, Invitrogen). For human insulin and B2M double-staining, the sections were stained with a guinea pig anti-human insulin primary antibody (1:200 dilution, Abcam) and rabbit anti-human B2M monoclonal primary antibody (1:100 dilution, Abcam), followed by an FITC-labeled goat anti-guinea pig secondary IgG (1:100 dilution, Abcam) and Texas red conjugated goat anti-rabbit secondary IgG (1:100 dilution, Santa Cruz Biotechnology, Santa Cruz, CA). All sections were mounted with a mounting medium containing DAPI and analyzed using fluorescence microscopy, as described above.

**Statistical analysis.** Data are presented as mean  $\pm$  SD. Statistical comparisons between two groups were evaluated by Student *t* test and corrected by one-way ANOVA for multiple comparisons using GraphPad Prism 5 (GraphPad Software, Inc., La Jolla, CA). A value of  $P < 0.05$  was considered to indicate statistical significance. A Mantel-Cox log-rank test was used to compare the percentage of animals that developed diabetes.

## RESULTS

### In vitro labeling of the islets and downregulation of B2M

#### Probe accumulation in human pancreatic islet cells.

For efficient downregulation of the target gene, *B2M*, it is necessary to ensure adequate intracellular accumulation of the probe. On the basis of our prior experience with islet labeling (25,27), we incubated human islets with control and experimental probes for 48 h. Fluorescence microscopy showing excellent colocalization of the Cy5.5 signal with anti-dextran staining provided direct evidence that both probes were taken up by islet cells (Fig. 1). Further support for the probe accumulation was obtained by staining islets with Prussian blue for iron (Supplementary Fig. 3). Tiny blue dots in the cytoplasm of the islet cells represent clusters of nanoparticles, as described previously (26).

MTT assay performed on labeled islets showed that the treatment with the probes did not have any significant effect on islet viability (Supplementary Fig. 4A). Glucose-stimulated insulin secretion and the glucose-stimulation index were not affected in all treatment groups (Supplementary Fig. 4B and C).

**Silencing of B2M in vitro.** Silencing efficiency of the probes was evaluated after human islets were incubated with MN-siB2M or control MN-siSCR probe for 48 h. As revealed by real-time RT-PCR, the *B2M* mRNA expression in the islets incubated with the MN-siB2M probe was reduced by 37% relative to the control probe under basal conditions (Fig. 2A). The protein level was also decreased in MN-siB2M-treated islets, as shown by Western blot analysis (Fig. 2A). To mimic inflammatory conditions in vivo, islets were treated with human IFN- $\gamma$ , which produced a threefold increase of *B2M* mRNA expression. In the islets treated with the MN-siB2M probe, *B2M* mRNA expression was reduced by 46% relative to controls under IFN- $\gamma$ -stimulated conditions (Fig. 2B). The protein level of B2M under IFN- $\gamma$ -stimulated conditions was also decreased in MN-siB2M-treated islets, as demonstrated by Western blot (Fig. 2B). Additional evidence for decreased protein expression was obtained with fluorescence microscopy that showed reduced levels of staining for B2M under these conditions (Fig. 2C).

Islet protein-stimulated ELISPOT was used to evaluate CD8<sup>+</sup> T-cell responsiveness against islet proteins. T cells were purified, and their purity was confirmed by FACS analysis (Supplementary Fig. 5). Immune responsiveness of CD8<sup>+</sup> T cells was determined by calculating the number of activated IFN- $\gamma$ -producing CD8<sup>+</sup> T cells treated with islet lysates. As shown in Fig. 2D, the number of CD8<sup>+</sup> T cells activated after incubation with islet lysates obtained from MN-siB2M-treated islets was significantly less than the number of activated CD8<sup>+</sup> T cells obtained after incubation with lysates from sham-treated islets or islets treated with the MN-siSCR probe ( $P < 0.05$ ).

#### In vivo protection of islet grafts from T-cell challenge

**Monitoring changes in graft volume after adoptive transfer by in vivo MRI.** As we have previously shown, MRI provides a reliable method for monitoring changes in graft volume over time (26,32). Here, we monitored the renal subcapsular islet grafts of experimental and control mice after the T-cell challenge, which was done 1 week after transplantation, when most of the initial graft loss had already occurred and the graft was relatively stabilized (data not shown) (26). As seen in Fig. 3, grafts could be identified

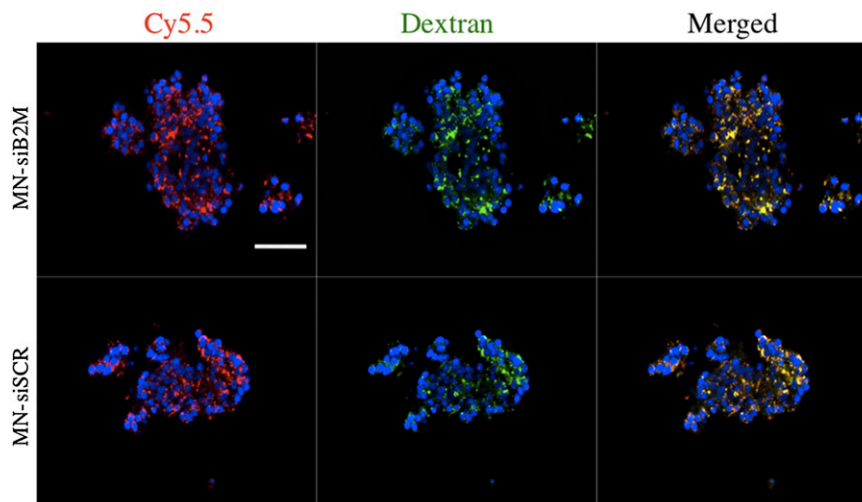


**FIG. 1.** Fluorescence microscopy of human islets after incubation with MN-siB2M or MN-siSCR probes for 48 h (red, Cy5.5; green, dextran; blue, DAPI nuclear stain). Colocalization of a Cy5.5 signal with anti-dextran staining provided direct evidence of the accumulation of both probes in islet cells (magnification bar = 50  $\mu$ m). (A high-quality digital representation of this figure is available in the online issue.)

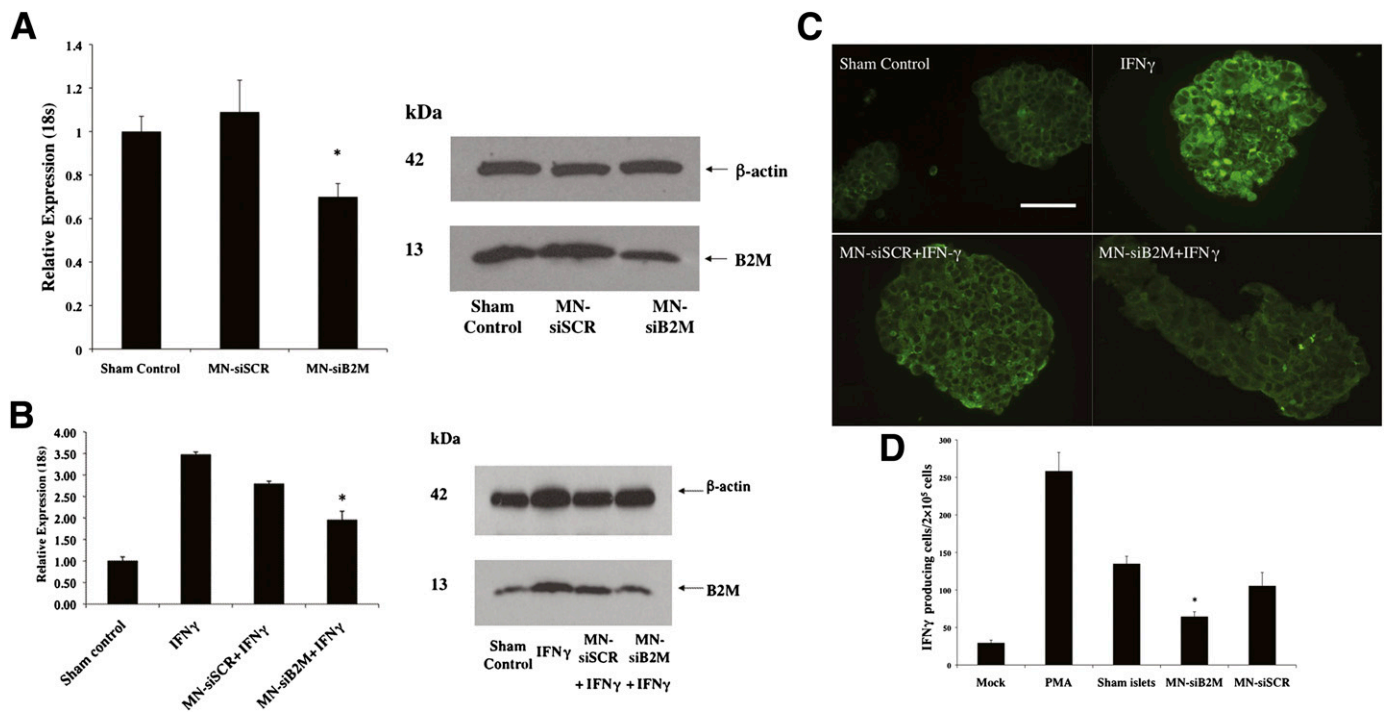


**FIG. 2.** Detection of downregulation of B2M expression by RT-PCR and Western blot. **A:** RT-PCR of human *B2M* mRNA expression in islets incubated with MN-siB2M or MN-siSCR probe for 48 h (\**P* < 0.05 compared with sham control) (*left*). Western blots showed decreased B2M protein levels in MN-siB2M-treated islets under basal conditions (*right*). **B:** RT-PCR of human *B2M* mRNA expression in islets treated with siRNA probes under IFN- $\gamma$ -stimulated conditions (\**P* < 0.05 compared with IFN- $\gamma$  treated islets) (*left*). Western blot showed a decreased level of B2M protein in MN-siB2M treated islets under IFN- $\gamma$  stimulated conditions (*right*). **C:** Fluorescence microscopy confirmed that the B2M expression in MN-siB2M-treated islets was significantly decreased under IFN- $\gamma$ -stimulated conditions compared with control and sham-treated islets (magnification bar = 50  $\mu$ m). **D:** Immune reactivity of primed splenocytes against islet proteins obtained after islet incubation with MN-siRNA probes as assessed by ELISPOT (\**P* < 0.05 compared with sham-treated or MN-siSCR-treated islets). (A high-quality digital representation of this figure is available in the online issue.)

on T2\*-weighted MRIs as pockets of signal loss disrupting the contour of the left kidney at the transplantation site. To correlate our findings, we used an alternative *in vivo* imaging modality to perform whole-body optical imaging of the same animals. Bright signal detected in the Cy5.5 channel originated from the mouse kidney, as was confirmed by 3D reconstruction of optical images and by the presence of the graft under the kidney capsule as shown postmortem (Supplementary Fig. 6 and Supplementary Videos 1 and 2).

To compare the relative changes of graft volumes between experimental and control groups, we performed a semiquantitative ROI analysis of T2 maps. As expected, graft volumes of experimental and control mice decreased after adoptive transfer. However, the rate of decrease in the experimental group was significantly lower than in the control group. This difference was pronounced, starting at 2 weeks after adoptive transfer and continuing for the duration of the experiment (*n* = 6, *P* < 0.05; Fig. 4A).

We expected to observe a delay in hyperglycemia caused by the T-cell challenge as a consequence of the preserved graft volume. MN-siB2M-labeled and control islets were initially transplanted in STZ-induced diabetic animals and successfully restored normoglycemia, indicating that their function was preserved after labeling (Supplementary Fig. 7). After T cell adoptive transfer, we observed the increase in blood glucose levels in both groups (Supplementary Fig. 7). However, animals transplanted with MN-siB2M-labeled islets developed diabetes, determined as blood glucose >250 mg/dL on two consecutive measurements, significantly later than the control group. As evident

from Kaplan-Meier analysis, diabetes developed at a mean of  $6.5 \pm 4.5$  days in the control group but was delayed up to  $23.8 \pm 4.8$  days in the experimental group (*P* = 0.0006, Fig. 4B). This study indicated that the protective effect of  $\beta$ 2M silencing allowed for the delay in diabetes development and for longer function of the grafts.

In the “no adoptive transfer” control group (*n* = 2) transplanted with MN-siB2M-labeled islets, normoglycemia was restored 3 days after transplantation. Neither mouse redeveloped diabetes for the duration of the study, demonstrating that labeling with the probe was safe long-term.

**Histologic correlation.** Animals were killed two weeks after adoptive transfer, and their kidneys were processed for fluorescence microscopy. Staining of kidney sections for B2M showed markedly reduced protein expression in MN-siB2M-treated grafts compared with controls, indicating effective silencing of the gene (Fig. 5A). This was accompanied by a notably lower infiltration of MN-siB2M-treated islet grafts with CD8<sup>+</sup> T cells compared with control grafts (Fig. 5B). Furthermore, Western blot analysis confirmed the reduction of B2M protein expression in the MN-siB2M-treated islet grafts compared with control grafts (Fig. 5C).

**DISCUSSION**

The major obstacle to successful islet transplantation is the potent T cell-mediated immune response occurring soon after the procedure that leads to  $\beta$ -cell damage (16).

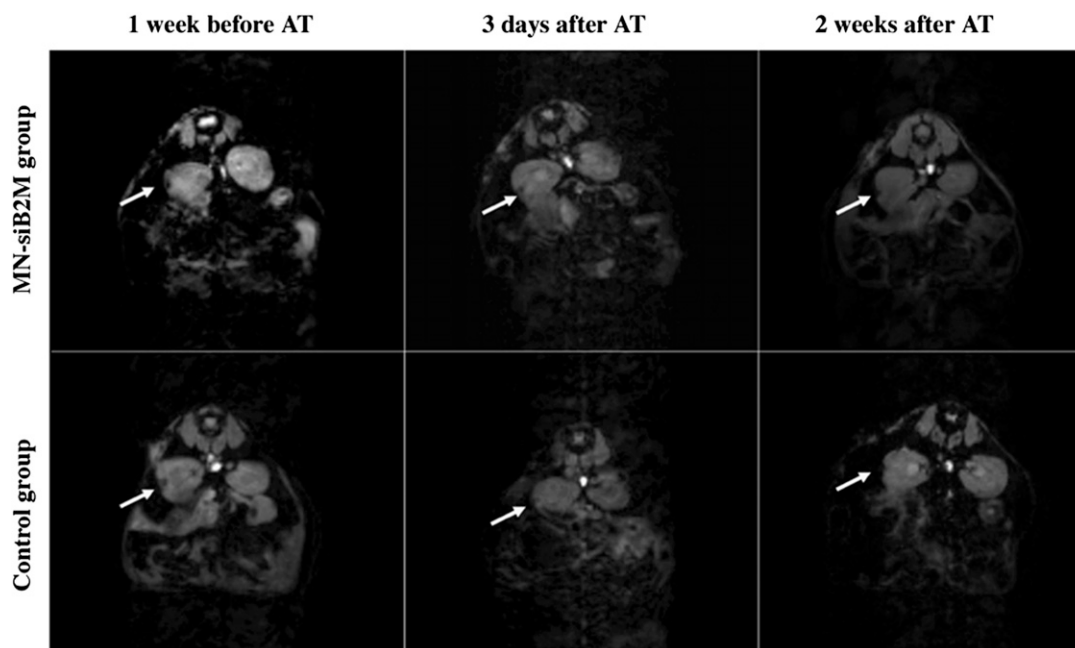


FIG. 3. Representative T2\* weighted MR images of grafts labeled with MN-siB2M or control probes under the left kidney capsule of NOD (B2M null)/*scid* mice 1 week before and 3 days and 2 weeks after adoptive transfer (AT) of T cells (white arrows indicate the islet graft areas).

The interaction between MHC class I molecules and CD8<sup>+</sup> T cells plays a major role in both allo- and xenograft rejection (33,34). MHC class I molecules are found on every nucleated cell of the body and consist of two components: the  $\alpha$  chain (the heavy chain) and B2M (the light chain). The  $\alpha$  chain and B2M are both essential for the proper folding of the entire MHC complex (35). Studies have shown that there is no detectable expression of MHC class I molecules on the surface of the cell in the absence of B2M (36).

We hypothesized that downregulation of B2M in pancreatic islet cells would lead to reduced recognition by T cells and, as a result, benefit the transplantation outcome. Therefore, the goal of our study was to downregulate B2M expression in human pancreatic islets before transplantation in B2M (null) NOD/*scid* mice using RNAi technology. We expected that aberrant expression of MHC class I proteins as the result of this downregulation would reduce or eliminate T cell recognition and provide the protection of pancreatic islet grafts in the xenotransplantation

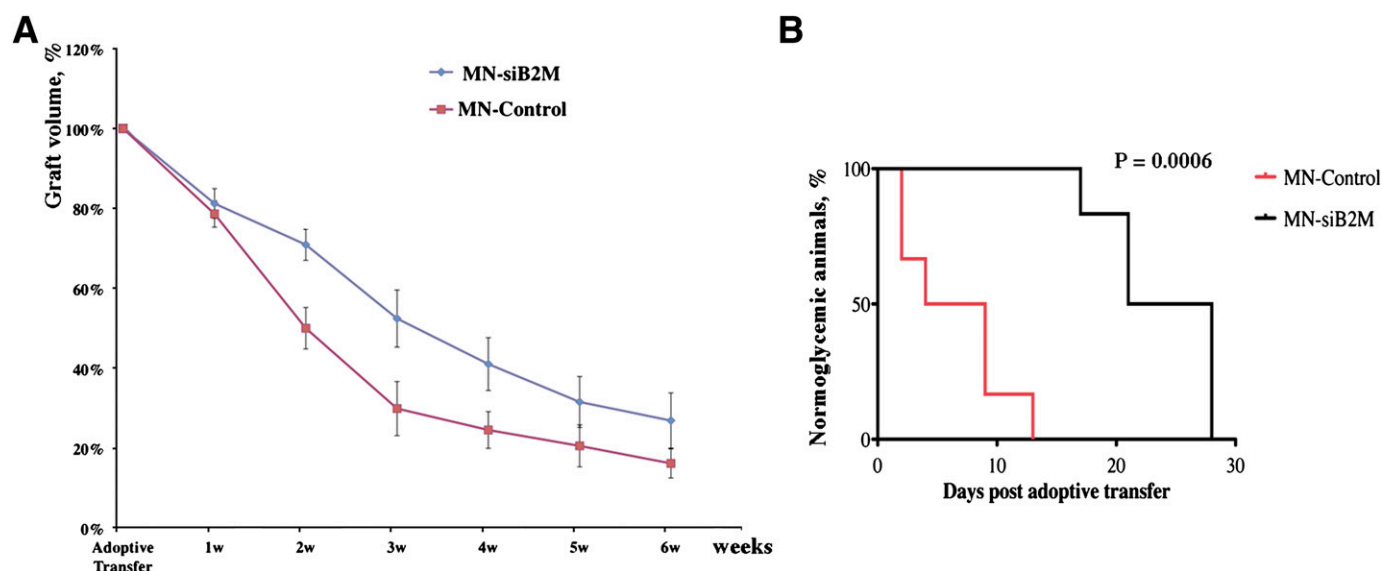
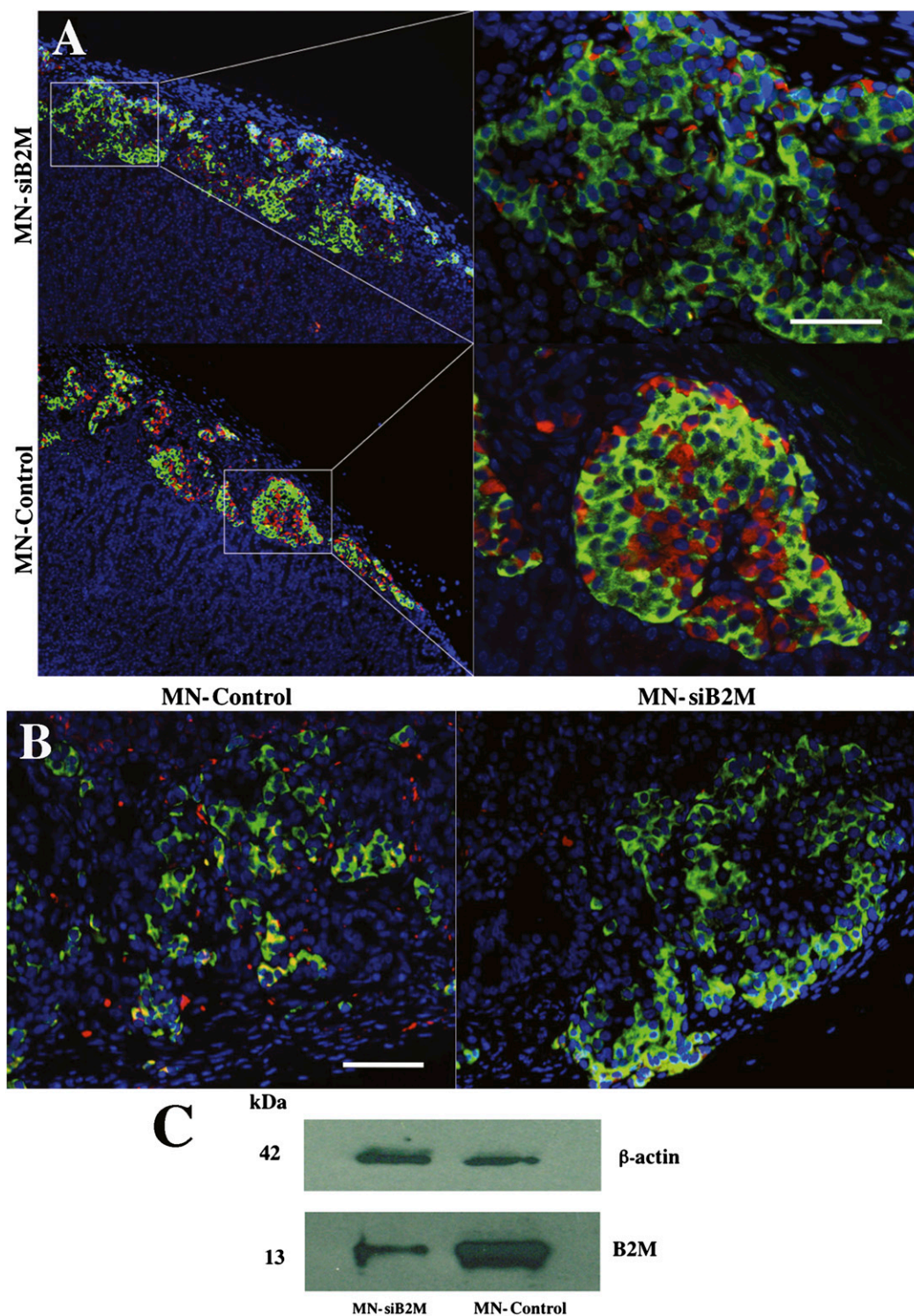


FIG. 4. **A:** Semiquantitative assessment of relative changes in graft volumes revealed the protective effect of MN-siB2M probe ( $n = 6$ ;  $P < 0.05$  starting 2 weeks after adoptive transfer compared with control group). **B:** Kaplan-Meier curve shows animals transplanted with control (red) and MN-siB2M-treated (black) islets. Development of diabetes was defined as the occurrence of hyperglycemia (blood glucose level  $>250$  mg/dL on two consecutive measurements,  $n = 6$ ;  $P = 0.0006$ ).



**FIG. 5.** *A:* Fluorescence microscopy revealed lower protein expression of B2M in MN-siB2M–treated grafts compared with control probe grafts 2 weeks after adoptive transfer (green, insulin; red, B2M; blue, DAPI nuclear stain; magnification bar = 50  $\mu$ m). *B:* Fluorescence microscopy showed markedly lower CD8<sup>+</sup> T-cell infiltration in MN-siB2M–treated grafts compared with control islet grafts 2 weeks after adoptive transfer (green, insulin; red, CD8; blue, DAPI nuclear stain; magnification bar = 40  $\mu$ m). *C:* Western blot analysis confirmed notably lower B2M protein expression in MN-siB2M–treated islet grafts compared with control grafts. (A high-quality digital representation of this figure is available in the online issue.)

model used in this study. To deliver siRNA to intact pancreatic islets, we used MNs that serve the dual function of acting as a siRNA delivery vehicle while also providing information by MRI assessment about changes in graft volume over time in vivo.

To mimic immune rejection of the xenografts, we used an adoptive transfer model in which islet grafts were severely challenged by exposure to a sudden onslaught of primed T cells isolated from the spleen of immunocompetent mice (37). These cells caused immune rejection and were

positively identified by histologic assessment (Fig. 5B) because B2M (null) NOD/*scid* mice lack endogenous CD8<sup>+</sup> T cells (38). Previous studies showed that 50% of the islet xenografts were rejected 9 days after transplantation without immunosuppression, with a mean survival time of  $10 \pm 2.1$  days (39). Downregulation of B2M expression in pancreatic islets led to significant protection of the grafts after adoptive transfer challenge. Diabetes development in this group occurred an average of 17 days later than in the control group. This was accompanied by a decline in graft volume in both groups, with the rate of this deterioration being significantly slower in the experimental group compared with the control group. MRI used in our study for estimation of graft volume is a modality with high spatial resolution, unlimited penetration through tissues, high tissue contrast, and tomographic capability. We have previously used it for the detection of graft reduction not only in the kidney capsule model of islet transplantation but also in a clinically approved model of islet grafting in the liver (25,26,31,32). Here, we demonstrate that *in vivo* MRI can serve as a tool for the determination of graft longevity during therapeutic intervention.

Clearly, our approach can potentially create a critical window of opportunity for the treatment of immune rejection and implementation of prompt intervention in a clinical scenario. Furthermore, it can be successfully applied to other situations where silencing MHC class I protein could be beneficial. For example, multiple studies have proven that this molecule also contributes to recurrence of autoimmune diabetes after islet transplantation in mice (40,41). The fact that B2M (null) NOD mice lacking CD8<sup>+</sup> T cells do not develop insulinitis implicates these cells as a crucial factor in the initiation of autoimmunity (42). Therefore, a B2M knockdown leading to targeted disruption of MHC class I molecule could potentially prevent autoimmunity in endogenous islets or autoimmune recurrence of T1DM in specific models of islet transplantation.

Immunosuppressive therapy can be toxic to transplanted islets and contribute to their progressive dysfunction (9,10). We believe that additional benefit from our current approach lies in the possibility of significantly reducing the dose of immunosuppressive therapy or ultimately avoiding the use of toxic immunosuppressants.

The major reason for the limited success of islet transplantation is a drastic decrease (up to 70%) of  $\beta$ -cell mass of the islet grafts during the first several weeks after transplantation (6,43); in fact, acute immune rejection begins as early as 1 week after transplantation. In our current study, we monitored the animals for 6 weeks after adoptive transfer, the period that most likely covered this initial damage. Our goal is to perform longitudinal studies in the future. In addition, we realize that despite B2M downregulation, the development of diabetes was not completely prevented but rather delayed. This is not unexpected, because factors other than infiltration of CD8<sup>+</sup> T cells contribute to immune rejection, including involvement of antigen-presenting cells expressing MHC class II molecules (44) as well as CD4<sup>+</sup> T cells (38), among others.

In addition, abolishing the recognition by CD8<sup>+</sup> T cells could lead to the activation of natural killer (NK) cells, which recognize and eliminate abnormal cells (45) through the interaction between the NK group 2D (NKG2D) and ligands on target cells. In this particular study, we transferred splenocytes from NOD mice (Supplementary Fig. 8), whose NK cells had a functional deficiency (46) and

therefore did not interfere with our observations. However, it should be possible to use our approach in the future to downregulate a variety of genes (including genes for NK cell ligands) responsible for islet damage by delivering a cocktail of nanoparticles or nanoparticles decorated with various sets of siRNAs.

In conclusion, to the best of our knowledge this is the first study that demonstrates the application of RNAi technology in combination with noninvasive imaging for the induction and detection of the delay in diabetes development caused by immune rejection in transplanted islets. We believe that this two-in-one theranostic approach could ultimately be applied in clinical settings for the protection of grafts in islet transplantation.

#### ACKNOWLEDGMENTS

This study was supported by National Institutes of Health Grants 5R01DK-080784 and R01DK-072137 to A.M.

No potential conflicts of interest relevant to this article were reported.

P.W. performed the *in vitro* experiments, animal surgery, and MRI scanning and participated in writing the manuscript. M.V.Y. synthesized the probe. C.R. assisted with optical imaging. A.R. and G.D. researched data. L.W. participated in animal studies. Z.M. participated in the experimental design. A.M. conceived the idea of the project and wrote the manuscript. A.M. is the guarantor of this work and, as such, had full access to all the data in the study and takes responsibility for the integrity of the data and the accuracy of the data analysis.

The authors thank Drs. James Markmann (Division of Transplantation, Department of Surgery, Massachusetts General Hospital) and Amol Kavishwar and Marytheresa Ifediba, MS (both from Molecular Imaging Laboratory, MGH/MIT/HMS Athinoula A. Martinos Center for Biomedical Imaging, Department of Radiology, Massachusetts General Hospital) for thoughtful discussions.

#### REFERENCES

1. The Diabetes Control and Complications Trial Research Group. The effect of intensive treatment of diabetes on the development and progression of long-term complications in insulin-dependent diabetes mellitus. *N Engl J Med* 1993;329:977–986
2. Fioretto P, Steffes MW, Sutherland DE, Goetz FC, Mauer M. Reversal of lesions of diabetic nephropathy after pancreas transplantation. *N Engl J Med* 1998;339:69–75
3. Troppmann C. Complications after pancreas transplantation. *Curr Opin Organ Transplant* 2010;15:112–118
4. Shapiro AM, Ricordi C, Hering BJ, et al. International trial of the Edmonton protocol for islet transplantation. *N Engl J Med* 2006;355:1318–1330
5. Alejandro R, Barton FB, Hering BJ, Wease S; Collaborative Islet Transplant Registry Investigators. 2008 Update from the Collaborative Islet Transplant Registry. *Transplantation* 2008;86:1783–1788
6. Barshes NR, Wyllie S, Goss JA. Inflammation-mediated dysfunction and apoptosis in pancreatic islet transplantation: implications for intrahepatic grafts. *J Leukoc Biol* 2005;77:587–597
7. Ricordi C, Strom TB. Clinical islet transplantation: advances and immunological challenges. *Nat Rev Immunol* 2004;4:259–268
8. Worcester Human Islet Transplantation Group. Autoimmunity after islet-cell allotransplantation. *N Engl J Med* 2006;355:1397–1399
9. Niclauss N, Bosco D, Morel P, Giovannoni L, Berney T, Parnaud G. Rapamycin impairs proliferation of transplanted islet  $\beta$  cells. *Transplantation* 2011;91:714–722
10. Zahr E, Molano RD, Pileggi A, et al. Rapamycin impairs *in vivo* proliferation of islet beta-cells. *Transplantation* 2007;84:1576–1583
11. Bouwman LH, Ling Z, Duinkerken G, Pipeleers DG, Roep BO. HLA incompatibility and immunogenicity of human pancreatic islet preparations

- cocultured with blood cells of healthy donors. *Hum Immunol* 2005;66:494–500
12. Rickels MR, Kamoun M, Kearns J, Markmann JF, Naji A. Evidence for allograft rejection in an islet transplant recipient and effect on beta-cell secretory capacity. *J Clin Endocrinol Metab* 2007;92:2410–2414
  13. Rickels MR, Kearns J, Markmann E, et al. HLA sensitization in islet transplantation. *Clin Transpl* 2006;413–420
  14. Eksler B, Ezzelarab M, Hara H, et al. Clinical xenotransplantation: the next medical revolution? *Lancet* 2012;379:672–683
  15. Lin CC, Ezzelarab M, Shapiro R, et al. Recipient tissue factor expression is associated with consumptive coagulopathy in pig-to-primate kidney xenotransplantation. *Am J Transplant* 2010;10:1556–1568
  16. Miranda V, Golshayan D, Read J, et al. Achieving permanent survival of islet xenografts by independent manipulation of direct and indirect T-cell responses. *Diabetes* 2005;54:1048–1055
  17. Zhan Y, Brady JL, Sutherland RM, Lew AM. Without CD4 help, CD8 rejection of pig xenografts requires CD28 costimulation but not perforin killing. *J Immunol* 2001;167:6279–6285
  18. Yi S, Feng X, Hawthorne W, Patel A, Walters S, O'Connell PJ. CD8+ T cells are capable of rejecting pancreatic islet xenografts. *Transplantation* 2000;70:896–906
  19. Fire A, Xu S, Montgomery MK, Kostas SA, Driver SE, Mello CC. Potent and specific genetic interference by double-stranded RNA in *Caenorhabditis elegans*. *Nature* 1998;391:806–811
  20. Figueiredo C, Seltsam A, Blasczyk R. Class-, gene-, and group-specific HLA silencing by lentiviral shRNA delivery. *J Mol Med (Berl)* 2006;84:425–437
  21. Haga K, Lemp NA, Logg CR, et al. Permanent, lowered HLA class I expression using lentivirus vectors with shRNA constructs: averting cytotoxicity by alloreactive T lymphocytes. *Transplant Proc* 2006;38:3184–3188
  22. Hacke K, Falahati R, Flebbe-Rehwaldt L, Kasahara N, Gaensler KM. Suppression of HLA expression by lentivirus-mediated gene transfer of siRNA cassettes and in vivo chemoselection to enhance hematopoietic stem cell transplantation. *Immunol Res* 2009;44:112–126
  23. Raper SE, Chirmule N, Lee FS, et al. Fatal systemic inflammatory response syndrome in a ornithine transcarbamylase deficient patient following adenoviral gene transfer. *Mol Genet Metab* 2003;80:148–158
  24. Hacein-Bey-Abina S, von Kalle C, Schmidt M, et al. A serious adverse event after successful gene therapy for X-linked severe combined immunodeficiency. *N Engl J Med* 2003;348:255–256
  25. Evgenov NV, Medarova Z, Dai G, Bonner-Weir S, Moore A. In vivo imaging of islet transplantation. *Nat Med* 2006;12:144–148
  26. Evgenov NV, Medarova Z, Pratt J, et al. In vivo imaging of immune rejection in transplanted pancreatic islets. *Diabetes* 2006;55:2419–2428
  27. Wang P, Yigit MV, Medarova Z, et al. Combined small interfering RNA therapy and in vivo magnetic resonance imaging in islet transplantation. *Diabetes* 2011;60:565–571
  28. Thomas HE, Parker JL, Schreiber RD, Kay TW. IFN-gamma action on pancreatic beta cells causes class I MHC upregulation but not diabetes. *J Clin Invest* 1998;102:1249–1257
  29. Toso C, Pawlick R, Lacotte S, et al. Detecting rejection after mouse islet transplantation utilizing islet protein-stimulated ELISPOT. *Cell Transplant* 2011;20:955–962
  30. Deeds MC, Anderson JM, Armstrong AS, et al. Single dose streptozotocin-induced diabetes: considerations for study design in islet transplantation models. *Lab Anim* 2011;45:131–140
  31. Medarova Z, Evgenov NV, Dai G, Bonner-Weir S, Moore A. In vivo multimodal imaging of transplanted pancreatic islets. *Nat Protoc* 2006;1:429–435
  32. Evgenov NV, Pratt J, Pantazopoulos P, Moore A. Effects of glucose toxicity and islet purity on in vivo magnetic resonance imaging of transplanted pancreatic islets. *Transplantation* 2008;85:1091–1098
  33. Ramirez-Victorino F, Beilke JN, Gill RG. Both innate and adaptive major histocompatibility complex class I-dependent immunity impair long-term islet xenograft survival. *Transplant Proc* 2008;40:557–558
  34. Markmann JF, Bassiri H, Desai NM, et al. Indefinite survival of MHC class I-deficient murine pancreatic islet allografts. *Transplantation* 1992;54:1085–1089
  35. Duprat E, Lefranc MP, Gascuel O. A simple method to predict protein-binding from aligned sequences—application to MHC superfamily and beta2-microglobulin. *Bioinformatics* 2006;22:453–459
  36. Hill DM, Kasliwal T, Schwarz E, et al. A dominant negative mutant beta 2-microglobulin blocks the extracellular folding of a major histocompatibility complex class I heavy chain. *J Biol Chem* 2003;278:5630–5638
  37. Alexander AM, Crawford M, Bertera S, et al. Indoleamine 2,3-dioxygenase expression in transplanted NOD islets prolongs graft survival after adoptive transfer of diabetogenic splenocytes. *Diabetes* 2002;51:356–365
  38. Christianson SW, Greiner DL, Hesselton RA, et al. Enhanced human CD4+ T cell engraftment in beta2-microglobulin-deficient NOD-scid mice. *J Immunol* 1997;158:3578–3586
  39. Triponez F, Oberholzer J, Morel P, et al. Xenogeneic islet re-transplantation in mice triggers an accelerated, species-specific rejection. *Immunology* 2000;101:548–554
  40. Young HY, Zucker P, Flavell RA, Jevnikar AM, Singh B. Characterization of the role of major histocompatibility complex in type 1 diabetes recurrence after islet transplantation. *Transplantation* 2004;78:509–515
  41. Serreze DV, Leiter EH, Christianson GJ, Greiner D, Roopenian DC. Major histocompatibility complex class I-deficient NOD-B2mnull mice are diabetes and insulinitis resistant. *Diabetes* 1994;43:505–509
  42. Pileggi A, Ricordi C, Alessiani M, Inverardi L. Factors influencing islet of Langerhans graft function and monitoring. *Clin Chim Acta* 2001;310:3–16
  43. Davalli AM, Ogawa Y, Ricordi C, Scharp DW, Bonner-Weir S, Weir GC. A selective decrease in the beta cell mass of human islets transplanted into diabetic nude mice. *Transplantation* 1995;59:817–820
  44. Coddington DA, Yang H, Rowden G, Colp P, Issekutz TB, Wright JR Jr. Islet allograft rejection in rats: a time course study characterizing adhesion molecule expression, MHC expression, and infiltrate immunophenotypes. *Cell Transplant* 1998;7:285–297
  45. Bauer S, Groh V, Wu J, et al. Activation of NK cells and T cells by NKG2D, a receptor for stress-inducible MICA. *Science* 1999;285:727–729
  46. Ogasawara K, Hamerman JA, Hsin H, et al. Impairment of NK cell function by NKG2D modulation in NOD mice. *Immunity* 2003;18:41–51